

Article

Testing the Interacting Dark Energy Model with Cosmic Microwave Background Anisotropy and Observational Hubble Data

Weiqiang Yang ^{1,*}, Lixin Xu ², Hang Li ³, Yabo Wu ¹ and Jianbo Lu ¹

¹ Department of Physics, Liaoning Normal University, Dalian 116029, China; ybwu61@163.com (Y.W.); lvjianbo819@163.com (J.L.)

² Institute of Theoretical Physics, School of Physics, Dalian University of Technology, Dalian 116024, China; lxxu@dlut.edu.cn

³ College of Medical Laboratory, Dalian Medical University, Dalian 116044, China; lh@dmu.edu.cn

* Correspondence: d11102004@mail.dlut.edu.cn

Received: 26 May 2017; Accepted: 23 June 2017; Published: 17 July 2017

Abstract: The coupling between dark energy and dark matter provides a possible approach to mitigate the coincidence problem of the cosmological standard model. In this paper, we assumed the interacting term was related to the Hubble parameter, energy density of dark energy, and equation of state of dark energy. The interaction rate between dark energy and dark matter was a constant parameter, which was, $Q = 3H\zeta(1 + w_x)\rho_x$. Based on the Markov chain Monte Carlo method, we made a global fitting on the interacting dark energy model from Planck 2015 cosmic microwave background anisotropy and observational Hubble data. We found that the observational data sets slightly favored a small interaction rate between dark energy and dark matter; however, there was not obvious evidence of interaction at the 1σ level.

Keywords: dark energy; interaction; observational constraint

1. Introduction

Dark energy theory could be used to explain late-time cosmic acceleration. A cosmological constant Λ with equation of state $w_\Lambda = -1$ is the simplest candidate of dark energy, which could be favored by the CMB data sets from Planck 2015 [1–3]; however, it is plagued with the fine-tuning problem and coincidence problem [4–6].

In order to avoid this coincidence problem, the time-varying cosmological constant model provides a possibility [7–15]. Besides, the unified dark fluid model and interacting dark energy model is suggested. All the theoretical models need to be tested by the observational data sets, and the cosmological constraint could identify the model parameter space. For the unified dark energy fluid model, it may be a mixture of dark energy and dark matter components, dubbed as dark degeneracy. In [16–18], the unified dark fluid with constant adiabatic sound speed α was tested by the cosmic microwave background (CMB) from WMAP7 (WMAP 7-year data) [19], baryon acoustic oscillation (BAO), type Ia supernovae (SNIa), the results showed a very small value of adiabatic sound speed, the order was about 10^{-3} in 1σ region. Another kind of unified model is the Chaplygin gas model and its generalized model, such as generalized Chaplygin gas, modified Chaplygin gas and so on, several work have been done to constrain the model parameter space of series of Chaplygin gas models [20–23], in [22], the model parameters of generalized Chaplygin gas were shown, $\alpha = 0.00126^{+0.000970+0.00268}_{-0.00126-0.00126}$ and $B_s = 0.775^{+0.0161+0.0307}_{-0.0161-0.0338}$. In [23], by using Markov Chain Monte Carlo method, a tight constraint was obtained: $\alpha = 0.000727^{+0.00142+0.00391}_{-0.00140-0.00234}$, $B = 0.000777^{+0.000201+0.000915}_{-0.000302-0.000697}$ and $B_s = 0.782^{+0.0163+0.0307}_{-0.0162-0.0329}$. The recent observational data sets did

not favor the phenomenon of fast transition of equation of state for the unified dark fluid model [24]. Moreover, when one considered the viscous effects in the Chaplygin gas model, the bulk viscosity coefficient parameter was constrained in the order of 10^{-5} [25,26]. For the above unified dark fluid model, one also could decompose it into dark matter interacting with vacuum energy. This kind of decomposed model has been constrained in [27,28], with the joint constraint from the geometry measurement and growth rate, the decomposed model parameter α is constrained in the order of 10^{-4} [28]. For the decomposed dark fluid model, the interaction between dark energy and dark matter might be naturally introduced without adding any additional degrees of freedom, this is a possibility of interaction between the dark sectors. Besides, one also could bring in dark coupling by some other mechanism, such as from the viewpoint of particle physics.

From a particle physics point of view, it would be natural to assume that these fields interact with each other or with dark matter [29–31]. However, in the cosmological standard model, dark matter and dark energy are assumed to feel only each others gravitational effects. In this paper, we relax this hypothesis by allowing for coupling between dark matter and dark energy, that is, a phenomenological energy transfer term in the dark fluids. The interacting dark energy could be adopted to avoid the coincidence problem. In the literature, there are two main categories for the choice of the phenomenological energy exchange term. A choice for a phenomenological interaction is a constant times either of the energy densities or some combination of them (without including the Hubble parameter and hence an implicit time dependence), as done for example in [32–39]. In another interacting dark energy model, Q is composed by the times of Hubble rate H , energy densities of dark fluids [40–65]. For this kind of interacting dark energy model, the main motivation is mainly from the phenomenological consideration, this could be found from the background conservation equation of dark energy or dark matter, the left-hand-side dimension of this equation is $H\rho_i$ ($i = c, x$), so one possible background energy transfer is proportional to $H\rho_i$. Some constraint results have been presented in the previous papers. Before Planck data, $Q = \Gamma_x\rho_x$ was considered in [38], the interacting dark energy with a constant equation of state has been constrained by CMB from WMAP7 [19], BAO, Hubble Space Telescope (HST) and SNIa, the results showed that the best-fit value of interaction rate was $\Gamma_x/H_0 = 0.366$. After Planck data, in [66], the perturbed expansion rate of the Universe and the interacting form $Q = H\zeta_x\rho_x$ was considered, this interacting model has been tested by CMB from Planck + WMAP9 [67,68] and BAO. The constraint results presented that the mean values of interaction rate was $\zeta_x = -0.61^{+0.12}_{-0.25}$ at 1σ level. The constraint results of energy exchange $Q = 3H\zeta\rho_x$ from CMB, BAO, SNIa, Redshift-space distortions (RSD) [69] have shown that the interaction rate was the order of 10^{-3} at 1σ level, there was no evidence for the coupling between dark energy and dark matter [41–44].

In this paper, we will test the model parameter space of interacting dark energy by CMB from Planck 2015 and observational Hubble data (OHD). The outline of this paper is as follows. Firstly, the modified background and perturbation equations of interacting dark energy will be shown. In the next two sections, we would look for the cosmological effects on the interaction rate and equation of state, and we list the data sets, and then make some analysis and discussion for the testing results and parameter contours. Finally, we present the conclusion of this paper.

2. The Basic Background and Perturbation Equations of Interacting Dark Energy Model

We treat the dark matter (c) and dark energy (x) as fluids that have equation of state parameters $w_c = 0$ and $w_x = p_x/\rho_x$, and the energy-exchange rate is Q , so the modified background equations for the individual components are

$$\rho'_c + 3\mathcal{H}\rho_c = aQ_c = -aQ, \quad (1)$$

$$\rho'_x + 3\mathcal{H}(1 + w_x)\rho_x = aQ_x = aQ, \quad (2)$$

where a prime indicates derivative with respect to conformal time τ , a is the scale factor of the Universe, $\mathcal{H} = a'/a$ is the conformal Hubble parameter.

In a general gauge, the perturbed Friedmann–Robertson–Walker (FRW) metric is [70]

$$ds^2 = a^2(\tau)\{- (1 + 2\phi)d\tau^2 + 2\partial_i B d\tau dx^i + [(1 - 2\psi)\delta_{ij} + 2\partial_i\partial_j E]dx^i dx^j\}, \tag{3}$$

where ϕ, B, ψ and E are the gauge-dependent scalar perturbations quantities.

The four-velocity of A fluid is given by $u_A^\mu = a^{-1}(1 - \phi, \partial^i v_A)$ [34,36,38,71], where v_A is the peculiar velocity potential whose relation with the volume expansion is $\theta_A = -k^2(v_A + B)$ in Fourier space [36,70]. With the interaction between the dark fluids, one knows that the energy-momentum conservation equation of A fluid becomes [34,36,38]

$$\nabla_\nu T_A^{\mu\nu} = Q_A^\mu, \quad \sum_A Q_A^\mu = 0, \tag{4}$$

where \tilde{Q}_A and F_A^μ , respectively, represent the energy and momentum transfer rate, relative to the four-velocity u^μ , one has $Q_A^\mu = \tilde{Q}_A u^\mu + F_A^\mu$ [34,36,38] where $\tilde{Q}_A = Q_A + \delta Q_A$ and $F_A^\mu = a^{-1}(0, \partial^i f_A)$, Q_A is the background term of the general interaction, and f_A is a momentum transfer potential. The perturbed energy-momentum transfer four-vector can be split as $Q_0^A = -a[Q_A(1 + \phi) + \delta Q_A]$ and $Q_i^A = a\partial_i[Q_A(v + B) + f_A]$ [34,36,38]. The perturbed energy and momentum balance equations are [34,36]

$$\delta\rho'_A + 3\mathcal{H}(\delta\rho_A + \delta p_A) - 3(\rho_A + p_A)\psi' - k^2(\rho_A + p_A)(v_A + E') = aQ_A\phi + a\delta Q_A, \tag{5}$$

$$\delta p_A + [(\rho_A + p_A)(v_A + B)]' + 4\mathcal{H}(\rho_A + p_A)(v_A + B) + (\rho_A + p_A)\phi - \frac{2}{3}k^2 p_A \pi_A = aQ_A(v + B) + af_A. \tag{6}$$

We specialize the momentum transfer potential as the simplest physical choice which is zero in the rest frame of dark matter [33,36,38] and assuming $\pi_A = 0$, so the momentum transfer potential is $k^2 f_A = Q_A(\theta - \theta_c)$. The pressure perturbation $\delta p_A = c_{sA}^2 \delta\rho_A + (c_{sA}^2 - c_{aA}^2)\rho'_A(v_A + B)$ [36,72] ($c_{aA}^2 = p'_A/\rho'_A = w_x + w'_x/(\rho'_A/\rho_A)$ is the adiabatic sound speed, and c_{sA}^2 is the A-fluid physical sound speed in the rest frame). When the non-adiabatic perturbation is considered, according to [72], it is convenient to separate out the non-adiabatic stress or entropy contribution which include the adiabatic sound speed and non-adiabatic pressure. The adiabatic sound speed is related to the equation of state. Meanwhile, one could assume the effective sound speed, it is also could be thought of as a rest frame sound speed which is physical and non-negative, for the intrinsic non-adiabatic perturbation in some fluid, the adiabatic sound speed and effective sound speed are different. However, with the assumption of pure adiabatic contribution to the perturbations, they are equal [22,73]. In the synchronous gauge ($\phi = B = 0, \psi = \eta$, and $k^2 E = -h/2 - 3\eta$), from the phenomenological consideration, for a constant equation of state w_x interacting dark energy with $Q = 3H\xi(1 + w_x)\rho_x$, the continuity and Euler equations for dark energy and dark matter are

$$\begin{aligned} \delta'_x &= -(1 + w_x) \left(\theta_x + \frac{h'}{2} \right) - 3\mathcal{H}(c_{sx}^2 - w_x) \left[\delta_x + 3\mathcal{H}(1 + w_x) \frac{\theta_x}{k^2} \right] \\ &+ 3\mathcal{H}\xi(1 + w_x) \left[\frac{\theta + h'/2}{3\mathcal{H}} + 3\mathcal{H}(c_{sx}^2 - w_x) \frac{\theta_x}{k^2} \right], \end{aligned} \tag{7}$$

$$\theta'_x = -\mathcal{H}(1 - 3c_{sx}^2)\theta_x + \frac{c_{sx}^2}{(1 + w_x)}k^2\delta_x + 3\mathcal{H}\xi \left[\theta_c - (1 + c_{sx}^2)\theta_x \right], \tag{8}$$

$$\delta'_c = - \left(\theta_c + \frac{h'}{2} \right) + 3\mathcal{H}\xi(1 + w_x) \frac{\rho_x}{\rho_c} \left(\delta_c - \delta_x - \frac{\theta + h'/2}{3\mathcal{H}} \right), \tag{9}$$

$$\theta'_c = -\mathcal{H}\theta_c, \tag{10}$$

where the Hubble rate H should be treated as a local variable in the energy exchange, $\delta\mathcal{H}/\mathcal{H} = (\theta + h'/2)/(3\mathcal{H})$ [40].

3. Cosmological Effects, Observational Data Sets and Fitting Results

When the interaction between the dark sectors is considered, some cosmological effects could take place, so we try to look for theoretical predictions of CMB temperature power spectra. When the interaction rate ξ_x is varied, the influences on the CMB temperature power spectra are presented in Figure 1. The different interaction rate ξ_x changes the effective density parameter of dark matter which will alter the sound horizon. As a result, the first peak of CMB temperature power spectra is modified. At large scales $l < 100$, the integrated Sachs–Wolfe (ISW) effect is dominant, the changed parameter ξ_x affects the CMB power spectra via ISW effect due to the evolution of gravitational potential. Meanwhile, we also show the cosmological effects of CMB power spectra for varied equations of state w_x in Figure 2.

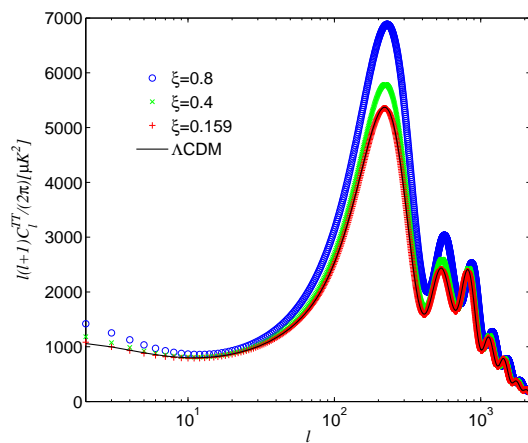


Figure 1. The cosmic microwave background (CMB) Temperature (TT) power spectra of an interacting dark energy model for varied interaction rate ξ , the other parameters are used the mean value from the CMB+ observational Hubble data (OHD) results of Table 1.

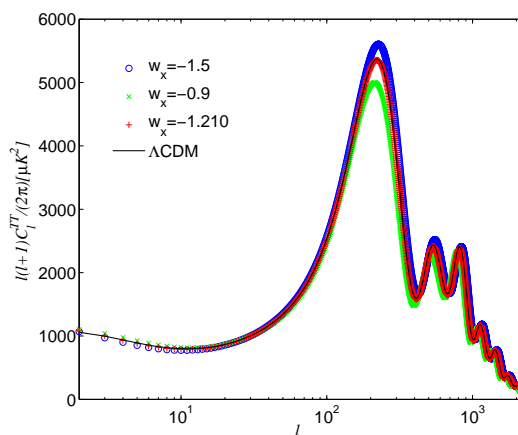


Figure 2. The CMB TT power spectra of interacting dark energy model for varied equation of state w_x , the other parameters used the mean value from the CMB + OHD results of Table 1.

We use the eight-dimensional parameter space of the interacting dark energy model,

$$P \equiv \{ \Omega_b h^2, \Omega_c h^2, \Theta_S, \tau, w_x, \xi, n_s, \log[10^{10} A_S] \} \tag{11}$$

where $\Omega_b h^2, \Omega_c h^2, \Theta_S, \tau, n_s, \log[10^{10} A_S]$ is the six basic parameters, ξ is the interaction rate which denotes the energy exchange rate between dark energy and dark matter, w_x is the equation of state

parameter of dark energy. The following priors of model parameters are used: $\Omega_b h^2 \in [0.005, 0.1]$, $\Omega_c h^2 \in [0.01, 0.99]$, $\Theta_s = 100\theta_{MC} \in [0.5, 10]$, $\tau \in [0.01, 0.8]$, $\zeta \in [0, 1]$, $w_x \in [-2, 0]$, $n_s \in [0.9, 1.1]$, $\log[10^{10} A_S] \in [2.7, 4]$. Here, we modify the public available codes CAMB [74] to calculate the CMB power spectra, and make the global fitting based on the cosmological Markov Chain Monte Carlo package CosmoMC [75].

In this paper, we just plan to test the model parameter space of interacting dark energy with CMB from Planck and OHD.

- CMB: The CMB data from Planck 2015 measurements [1,2] have been used in our analysis. Here, we combine the likelihood of full Planck temperature-only C_l^{TT} with the low- l polarization $C_l^{TE} + C_l^{EE} + C_l^{BB}$, which in notation is the same as the “PlanckTT + lowP” of [3].
- OHD: The cosmic chronometer approach is a method to determine the Hubble parameter values at different redshifts with the use of most massive and passively evolving galaxies in our universe. These galaxies are known as cosmic chronometers. The idea is to determine dz/dt and hence the Hubble parameter $H(z) = -1/(1+z)dz/dt$. Since the measurement of dz is obtained through the spectroscopic method with high accuracy, a precise measurement of the Hubble parameter lies on the precise measurement of the differential age evolution dt of such galaxies, and hence these measurements are considered to be model independent. In [76], Moresco et al. extract a sample of more than 130,000 of the most massive and passively evolving galaxies, obtaining five new cosmology-independent $H(z)$ measurements in the redshift range $0.3 < z < 0.5$, with an accuracy of $\sim 11\text{--}16\%$ incorporating both statistical and systematic errors. Once combined, these measurements yield a 6% accuracy constraint of $H(z = 0.4293) = 91.8 \pm 5.3$ km/s/Mpc. This analysis highlights the wide potential of the cosmic chronometers approach: it permits us to derive constraints on the expansion history of the Universe with results that are competitive with standard probes. Moreover, most importantly, the estimates are independent of the cosmological model, so it can constrain the cosmological beyond and including the Λ CDM model. A detailed description about the cosmic chronometer method can be found in [76]. Here, we use 30 data points of the Hubble parameter in the redshift interval $0 < z < 2$ [76].

Firstly, we make an analysis of the constraint results. In Table 1, we have listed the global fitting results of the interacting dark energy model. The one-dimensional (1D) marginalized posterior distribution on individual parameters and 2D marginalized posterior distribution contours are shown in Figure 3. For the single constraint from the Planck 2015 CMB data, the testing results of interaction rate and equation of state are, respectively, $\zeta = 0.149^{+0.040+0.241}_{-0.149-0.149}$ and $w_x = -1.249^{+0.082+0.179}_{-0.080-0.165}$ in 2σ region. For the joint constraint from Planck 2015 CMB and OHD, the results are $\zeta = 0.159^{+0.045+0.216}_{-0.159-0.159}$ and $w_x = -1.210^{+0.078+0.127}_{-0.066-0.134}$. The OHD simply provides a geometrical constraint for the background evolution of this interacting dark energy model. Concretely, from the background equations, we could calculate the numerical solution for the energy density of dark energy and dark matter at different redshifts. Under this situation, the pure geometrical measurement from OHD would provide weak constraint on the interacting dark energy model. This opinion could be seen from the Table 1. After adding the constraint from the observational Hubble data, the testing results have not been improved. The observational data sets, CMB and OHD, slightly favor a small interaction rate between dark energy and dark matter. Recent developments in model independent techniques of cosmic reconstruction seem to indicate that w is not smaller than -1 [77,78]. Meanwhile, from our constraint results of the interacting dark energy model, the mean value of the equation of state is less than -1 and it shows a phantom phrase, which might be because of our choice of interaction form with the equation of state factor $(1 + w_x)$.

Table 1. The mean values with 1, 2, 3 σ errors and best-fit value of the model parameters and derived cosmological parameters for an interacting dark energy model, where “CMB” and “CMB + OHD” denotes the mean values with error bars and best-fit value from constraint results of CMB and CMB + OHD.

Parameters	Mean with Errors (CMB)	Best Fit (CMB)	Mean with Errors (CMB + OHD)	Best Fit (CMB + OHD)
$\Omega_c h^2$	0.1314 $^{+0.0064 + 0.0191 + 0.0225}_{-0.0130 - 0.0150 - 0.0173}$	0.1409	0.1304 $^{+0.0065 + 0.0167 + 0.0208}_{-0.0113 - 0.0142 - 0.0164}$	0.1434
$\Omega_b h^2$	0.02216 $^{+0.00023 + 0.00049 + 0.00066}_{-0.00024 - 0.00046 - 0.00061}$	0.02220	0.02220 $^{+0.00021 + 0.00040 + 0.00052}_{-0.00020 - 0.00040 - 0.00054}$	0.02229
$100\theta_{MC}$	1.03978 $^{+0.000694 + 0.00130 + 0.00160}_{-0.00070 - 0.00134 - 0.00168}$	1.03925	1.03990 $^{+0.00068 + 0.00118 + 0.00151}_{-0.00070 - 0.00117 - 0.00150}$	1.03933
τ	0.074 $^{+0.020 + 0.042 + 0.053}_{-0.020 - 0.040 - 0.050}$	0.085	0.077 $^{+0.018 + 0.037 + 0.046}_{-0.018 - 0.040 - 0.050}$	0.086
n_s	0.9724 $^{+0.0063 + 0.0116 + 0.0149}_{-0.0061 - 0.0120 - 0.0149}$	0.9750	0.9729 $^{+0.0054 + 0.0106 + 0.0139}_{-0.0054 - 0.0109 - 0.0143}$	0.9742
$\ln(10^{10} A_s)$	3.094 $^{+0.040 + 0.083 + 0.101}_{-0.040 - 0.077 - 0.097}$	3.115	3.099 $^{+0.036 + 0.070 + 0.087}_{-0.035 - 0.077 - 0.096}$	3.117
w_x	-1.249 $^{+0.082 + 0.179 + 0.202}_{-0.080 - 0.165 - 0.241}$	-1.257	-1.210 $^{+0.078 + 0.127 + 0.151}_{-0.066 - 0.134 - 0.166}$	-1.279
ξ	0.149 $^{+0.040 + 0.241 + 0.304}_{-0.149 - 0.149 - 0.149}$	0.268	0.159 $^{+0.045 + 0.216 + 0.331}_{-0.159 - 0.159 - 0.159}$	0.269
Ω_{m0}	0.288 $^{+0.020 + 0.048 + 0.058}_{-0.027 - 0.041 - 0.050}$	0.310	0.294 $^{+0.019 + 0.041 + 0.053}_{-0.022 - 0.039 - 0.048}$	0.312
σ_8	0.819 $^{+0.067 + 0.094 + 0.104}_{-0.043 - 0.113 - 0.123}$	0.767	0.815 $^{+0.058 + 0.084 + 0.096}_{-0.040 - 0.098 - 0.114}$	0.765
H_0	73.17 $^{+1.85 + 4.01 + 4.86}_{-1.87 - 3.66 - 4.46}$	72.68	72.25 $^{+1.63 + 3.27 + 4.42}_{-1.82 - 3.31 - 4.04}$	72.91

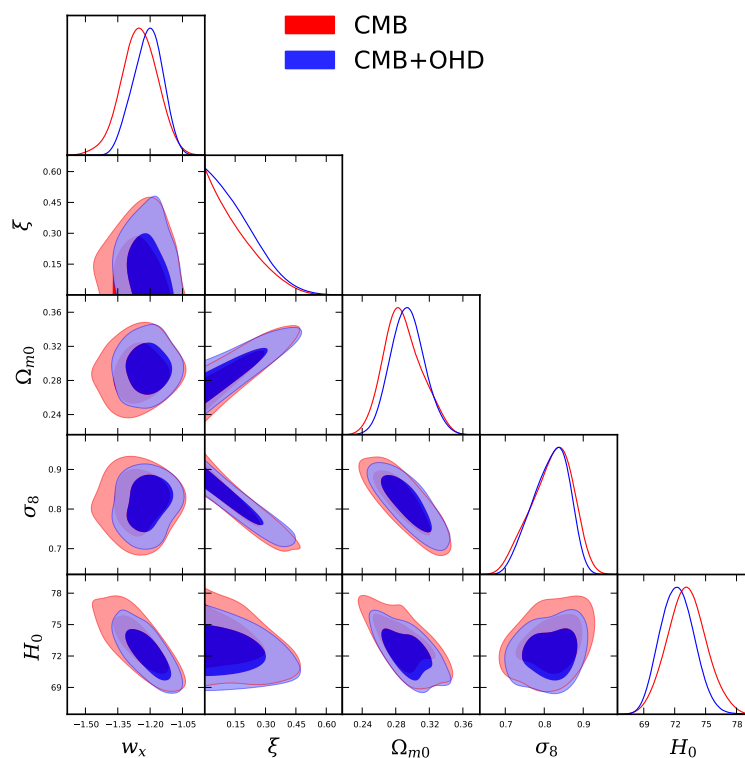


Figure 3. The 1D marginalized distribution on individual parameters and 2D contours of Model I $Q = 3H\xi(1 + w_x)\rho_x$ at 1 σ , 2 σ , 3 σ regions, the red contour is from the constraint of alone CMB from Planck 2015, the blue contour is from the joint constraint from CMB and OHD.

4. Conclusions

Current astronomical observations provide us with effective tools to study the possible interaction between dark energy and dark matter. In this paper, we considered the interacting dark energy model with a constant interaction rate. The background exchange transfer was related to the Hubble parameter, energy density of dark energy, and equation of state of dark energy, which was, $Q =$

$3H\zeta(1+w_x)\rho_x$. Based on the Markov chain Monte Carlo method, we adopted the CMB from Planck 2015, OHD data sets to test the parameter space of the interacting dark energy model. For the single constraint from the Planck 2015 microwave background anisotropy, the testing results of interaction rate and equation of state were, respectively, $\zeta = 0.149^{+0.040+0.241}_{-0.149-0.149}$ and $w_x = -1.249^{+0.082+0.179}_{-0.080-0.165}$ in 2σ region. For the joint constraint from Planck 2015 microwave background anisotropy and observational Hubble data, the results were $\zeta = 0.159^{+0.045+0.216}_{-0.159-0.159}$ and $w_x = -1.210^{+0.078+0.127}_{-0.066-0.134}$. After adding the constraint from the observational Hubble data, the testing results have not been obviously improved. The observational data sets, microwave background anisotropy and observational Hubble data slightly favor a small interaction rate between dark energy and dark matter. However, in the light of the testing results of interaction rate, we did not seek out any strong evidence for the existence of coupling between dark energy and dark matter, even at 1σ level. It was believed that there was no obvious evidence for the interacting dark energy models beyond the standard Λ CDM model from the point of view of possible interaction.

Acknowledgments: Weiqiang Yang's work is supported by the National Natural Science Foundation of China under Grant No. 11647153, the Foundation of Education Department of Liaoning Province in China under Grant No. L201683666. Lixin Xu's work is supported by the National Natural Science Foundation of China under Grant No. 11675032, "the Fundamental Research Funds for the Central Universities" under Grant No. DUT16LK31. Hang Li's work is supported by the National Natural Science Foundation of China under Grant No. 81601855, the Natural Science Foundation of Liaoning Province in China under Grant No. L2016036. Yabo Wu's work is supported by the National Natural Science Foundation of China under Grant No. 11575075. Jianbo Lu's work is supported by the National Natural Science Foundation of China under Grant No. 11645003.

Author Contributions: Weiqiang Yang and Lixin Xu calculated the formula and made the data analysis; Weiqiang Yang and Hang Li wrote the paper; Yabo Wu and Jianbo Lu gave some helpful suggestions to improve this paper. All authors have read and approved the final manuscript.

Conflicts of Interest: The authors declare no conflict of interest.

References

- Adam, R.; Ade, P.A.R.; Aghanim, N.; Armitage-Caplan, C.; Arnaud, M.; Ashdown, M.; Atrio-Barandela, F.; Aumont, J.; Aussel, H.; Baccigalupi, C.; et al. Planck 2015 results. I. Overview of products and scientific results. *Astron. Astrophys.* **2016**, *594*, doi:10.1051/0004-6361/201527101.
- Aghanim, N.; Arnaud, M.; Ashdown, M.; Aumont, J.; Baccigalupi, C.; Banday, A.J.; Barreiro, R.B.; Bartlett, J.G.; Bartolo, N.; Battaner, E.; et al. Planck 2015 results. XI. CMB power spectra, likelihoods, and robustness of parameters. *Astron. Astrophys.* **2016**, *594*, doi:10.1051/0004-6361/201526926.
- Ade, P.A.R.; Aghanim, N.; Arnaud, M.; Aumont, J.; Baccigalupi, C.; Banday, A.J.; Barreiro, R.B.; Bartlett, J.G.; Bartolo, N.; Battaner, E.; et al. Planck 2015 results. XIII. Cosmological parameters. *Astron. Astrophys.* **2016**, *594*, doi:10.1051/0004-6361/201525830.
- Weinberg, S. The Cosmological Constant Problem. *Rev. Mod. Phys.* **1989**, doi:10.1103/RevModPhys.61.1.
- Carroll, S.M. The Cosmological Constant. *arXiv* **2001**, arXiv:astro-ph/0004075.
- Zlatev, I.; Wang, L.; Steinhardt, P.J. Quintessence, Cosmic Coincidence, and the Cosmological Constant. *Phys. Rev. Lett.* **1999**, *82*, 896–899.
- Dymnikova, I.; Khlopov, M.Y. Decay of cosmological constant as Bose condensate evaporation. *Mod. Phys. Lett. A* **2000**, *15*, 2305–2314.
- Dymnikova, I.; Khlopov, M.Y. Decay of cosmological constant in self-consistent inflation. *Eur. Phys. J. C* **2001**, *20*, 139–146.
- Ray, S.; Khlopov, M.Y.; Ghosh, P.P.; Mukhopadhyay, U. Phenomenology of Λ -CDM model: A possibility of accelerating Universe with positive pressure. *Int. J. Theor. Phys.* **2011**, *50*, 939–951.
- Doroshkevich, A.G.; Khlopov, M.Y.; Klypin, A.A. Large-scale structure formation by decaying massive neutrinos. *Mon. Not. R. Astr. Soc.* **1989**, *239*, 923–938.
- Wang, W.; Gui, Y.-X.; Xu, L.; Lu, J. The Integrated Sachs–Wolfe Effect in Time Varying Vacuum Model. *Phys. Rev. D* **2010**, *81*, 083514.
- Xu, L. Time Variable Cosmological Constant from Renormalization Group Equations. *Mod. Phys. Lett. A* **2010**, *25*, 377–388.

13. Xu, L.; Lu, J.; Li, W. Time Variable Cosmological Constants from the Age of Universe. *Phys. Lett. B* **2010**, *690*, 333–336.
14. Xu, L.; Lu, J.; Li, W. Time Variable Cosmological Constants from Cosmological Horizons. *arXiv* **2010**, arXiv:0905.4772.
15. Xu, L.; Wang, Y.; Noh, H. CMB Temperature and Matter Power Spectrum in a Decay Vacuum Dark Energy Model. *Phys. Rev. D* **2011**, *84*, 123004.
16. Xu, L. Unified Dark Fluid with Constant Adiabatic Sound Speed and Cosmic Constraints. *Phys. Rev. D* **2012**, *85*, 043003.
17. Xu, L. Unified Dark Fluid with Constant Adiabatic Sound Speed: Including Entropic Perturbations. *Phys. Rev. D* **2013**, *87*, 043503.
18. Xu, L. Spherical Collapse of a Unified Dark Fluid with Constant Adiabatic Sound Speed. *Eur. Phys. J. C* **2013**, *73*, 2344.
19. Komatsu, E.; Smith, K.M.; Dunkley, J.; Bennett, C.L.; Gold, B.; Hinshaw, G.; Jarosik, N.; Larson, D.; Nolte, M.R.; Page, L.; et al. Seven-Year Wilkinson Microwave Anisotropy Probe (WMAP) Observations: Cosmological Interpretation. *Astrophys. J. Suppl. Ser.* **2011**, *192*, 18.
20. Lu, J.; Geng, D.; Xu, L.; Wu, Y.; Liu, M. Reduced modified Chaplygin gas cosmology. *arXiv* **2015**, arXiv:1312.0779.
21. Xu, L.; Lu, J. Cosmological constraints on generalized Chaplygin gas model: Markov Chain Monte Carlo approach. *arXiv* **2010**, arXiv:1004.3344.
22. Xu, L. Revisiting Generalized Chaplygin Gas as a Unified Dark Matter and Dark Energy Model. *Eur. Phys. J. C* **2012**, *72*, 1883.
23. Xu, L. Modified Chaplygin Gas as a Unified Dark Matter and Dark Energy Model and Cosmic Constraints. *Eur. Phys. J. C* **2012**, *72*, 1931.
24. Yang, W.; Xu, L. Unified dark fluid with fast transition: Including entropic perturbations. *Phys. Rev. D* **2013**, *88*, 023505.
25. Li, W.; Xu, L. Spherical top-hat Collapse of a Viscous Unified Dark Fluid. *Eur. Phys. J. C* **2014**, *74*, 2870.
26. Li, W.; Xu, L. Viscous Generalized Chaplygin Gas as a Unified Dark Fluid: Including Perturbation of Bulk Viscosity. *Eur. Phys. J. C* **2014**, *74*, 2765.
27. Wang, Y.; Wands, D.; Xu, L.; De-Santiago, J.; Hojjati, A. Cosmological constraints on a decomposed Chaplygin gas. *Phys. Rev. D* **2013**, *87*, 083503.
28. Yang, W.; Xu, L.; Wang, Y.; Wu, Y. Constraints on a decomposed dark fluid with constant adiabatic sound speed by jointing the geometry test and growth rate after Planck data. *Phys. Rev. D* **2014**, *89*, 043511.
29. Baldi, M.; Salucci, P. Constraints on interacting dark energy models from galaxy Rotation Curves. *arXiv* **2012**, arXiv:1111.3953.
30. Amendola, L.; Quartin, M.; Tsujikawa, S.; Waga, I. Challenges for scaling cosmologies. *Phys. Rev. D* **2006**, *74*, 023525.
31. Amendola, L. Linear and non-linear perturbations in dark energy models. *Phys. Rev. D* **2004**, *69*, 103524.
32. Song, Y.-S.; Hollenstein, L.; Caldera-Cabral, G.; Koyama, K. Theoretical Priors On Modified Growth Parametrisations. *arXiv* **2010**, arXiv:1001.0969.
33. Koyama, K.; Maartens, R.; Song, Y.-S. Velocities as a probe of dark sector interactions. *arXiv* **2009**, arXiv:0907.2126.
34. Majerotto, E.; Valiviita, J.; Maartens, R. Adiabatic initial conditions for perturbations in interacting dark energy models. *Mon. Not. R. Astron. Soc.* **2010**, *402*, 2344–2354.
35. Valiviita, J.; Maartens, R.; Majerotto, E. Observational constraints on an interacting dark energy model. *Mon. Not. R. Astron. Soc.* **2010**, *402*, 2355–2368.
36. Valiviita, J.; Majerotto, E.; Maartens, R. Large-scale instability in interacting dark energy and dark matter fluids. *arXiv* **2008**, arXiv:0804.0232.
37. Jackson, B.M.; Taylor, A.; Berera, A. On the large-scale instability in interacting dark energy and dark matter fluids. *Phys. Rev. D* **2009**, *79*, 043526.
38. Clemson, T.; Koyama, K.; Zhao, G.-B.; Maartens, R.; Valiviita, J. Interacting Dark Energy—Constraints and degeneracies. *Phys. Rev. D* **2012**, *85*, 043007.
39. Bean, R.; Flanagan, E.E.; Trodden, M. Adiabatic instability in coupled dark energy-dark matter models. *Phys. Rev. D* **2008**, *78*, 023009.

40. Gavela, M.B.; Honorez, L.L.; Mena, O.; Rigolin, S. Dark Coupling and Gauge Invariance. *arXiv* **2010**, arXiv:1005.0295.
41. Yang, W.; Xu, L. Cosmological constraints on interacting dark energy with redshift-space distortion after Planck data. *Phys. Rev. D* **2014**, *89*, 083517.
42. Yang, W.; Xu, L. Testing coupled dark energy with large scale structure observation. *arXiv* **2010**, arXiv:1401.5177.
43. Yang, W.; Xu, L. Coupled dark energy with perturbed Hubble expansion rate. *Phys. Rev. D* **2014**, *90*, 083532.
44. Yang, W.; Li, H.; Wu, Y.; Lu, J. Cosmological constraints on coupled dark energy. *arXiv* **2016**, arXiv:1608.07039.
45. Salvatelli, V.; Said, N.; Bruni, M.; Melchiorri, A.; Wands, D. Indications of a late-time interaction in the dark sector. *Phys. Rev. Lett.* **2014**, *113*, 181301.
46. He, J.-H.; Wang, B. Effects of the interaction between dark energy and dark matter on cosmological parameters. *arXiv* **2008**, arXiv:0801.4233.
47. Wang, B.; Abdalla, E.; Atrio-Barandela, F.; Pavon, D. Dark Matter and Dark Energy Interactions: Theoretical Challenges, Cosmological Implications and Observational Signatures. *Rep. Prog. Phys.* **2016**, *79*, 9.
48. Pu, B.-Y.; Xu, X.-D.; Wang, B.; Abdalla, E. Early dark energy and its interaction with dark matter. *Phys. Rev. D* **2015**, *92*, 123537.
49. Wang, Y.; Zhao, G.-B.; Wands, D.; Pogosian, L.; Crittenden, R.G. Reconstruction of the dark matter-vacuum energy interaction. *Phys. Rev. D* **2015**, *92*, 103005.
50. Nunes, R.C.; Pan, S.; Saridakis, E.N. New constraints on interacting dark energy from cosmic chronometers. *Phys. Rev. D* **2016**, *94*, 023508.
51. Xia, D.-M.; Wang, S. Constraining interacting dark energy models with latest cosmological observations. *Mon. Not. R. Astron. Soc.* **2016**, *463*, 952–956.
52. Mukherjee, A.; Banerjee, N. In search of the dark matter dark energy interaction: A kinematic approach. *Class. Quantum Grav.* **2017**, *34*, 035016.
53. Bhatia, A.S.; Sur, S. Phase Plane Analysis of Metric-Scalar Torsion Model for Interacting Dark Energy. *arXiv* **2016**, arXiv:1611.06902.
54. Ebrahimi, E.; Golchin, H.; Mehrabi, A.; Movahed, S.M.S. Consistency of nonlinear interacting ghost dark energy with recent observations. *arXiv* **2017**, arXiv:1611.06551.
55. Sharov, G.S.; Bhattacharya, S.; Pan, S.; Nunes, R.C.; Chakraborty, S. Generalized Ghost Dark Energy with Non-Linear Interaction. *arXiv* **2017**, arXiv:1701.00780.
56. Kumar, S.; Nunes, R.C. Echo for interaction in the dark sector. *arXiv* **2017**, arXiv:1702.02143.
57. Begue, D.; Stahl, C.; Xue, S.-S. A model of interacting dark fluids tested with supernovae data. *arXiv* **2017**, arXiv:1702.03185.
58. Yang, W.; Baneerjee, N.; Pan, S. Constraining a dark matter and dark energy interaction scenario with a dynamical equation of state. *arXiv* **2017**, arXiv:1705.09278.
59. Van de Bruck, C.; Mifsud, J.; Morrice, J. Testing coupled dark energy models with their cosmological background evolution. *Phys. Rev. D* **2017**, *95*, 043513.
60. Van de Bruck, C.; Mifsud, J.; Mimoso, J.P.; Nunes, N.J. Generalized dark energy interactions with multiple fluids. *arXiv* **2016**, arXiv:1605.03834.
61. Brax, P.; van de Bruck, C.; Martin, J. Anne-Christine Davis, Decoupling Dark Energy from Matter. *arXiv* **2009**, arXiv:0904.3471.
62. Brax, P.; van de Bruck, C.; Hall, L.M.H.; Weller, J.M. Slow-Roll Inflation in the Presence of a Dark Energy Coupling. *Phys. Rev. D* **2009**, *79*, 103508.
63. Brookfield, A.W.; van de Bruck, C.; Hall, L.M.H. New interactions in the dark sector mediated by dark energy. *Phys. Rev. D* **2008**, *77*, 043006.
64. Boehmer, C.G.; Caldera-Cabral, G.; Chan, N.; Lazkoz, R.; Maartens, R. Quintessence with quadratic coupling to dark matter. *Phys. Rev. D* **2010**, *81*, 083003.
65. Boehmer, C.G.; Caldera-Cabral, G.; Lazkoz, R.; Maartens, R. Dynamics of dark energy with a coupling to dark matter. *Phys. Rev. D* **2008**, *78*, 023505.
66. Salvatelli, V.; Marchini, A.; Lopez-Honorez, L.; Mena, O. New constraints on Coupled Dark Energy from Planck. *Phys. Rev. D* **2013**, *88*, 023531.

67. Ade, P.A.R.; Aghanim, N.; Armitage-Caplan, C.; Arnaud, M.; Ashdown, M.; Atrio-Barandela, F.; Aumont, J.; Baccigalupi, C.; Banday, A.J.; Barreiro, R.B.; et al. Planck 2013 results. XVI. Cosmological parameters. *arXiv* **2014**, arXiv:1303.5076.
68. Hinshaw, G.; Larson, D.; Komatsu, E.; Spergel, D.N.; Bennett, C.L.; Dunkley, J.; Nolta, M.R.; Halpern, M.; Hill, R.S.; Odegard, N.; et al. Nine-Year Wilkinson Microwave Anisotropy Probe (WMAP) Observations: Cosmological Parameter Results. *Astrophys. J. Suppl.* **2013**, *2008*, 2.
69. Samushia, L.; Reid, B.A.; White, M.; Percival, W.J.; Cuesta, A.J.; Lombriser, L.; Manera, M.; Nichol, R.C.; Schneider, D.P.; Bizyaev, D.; et al. The Clustering of Galaxies in the SDSS-III DR9 Baryon Oscillation Spectroscopic Survey: Testing Deviations from Λ and General Relativity using anisotropic clustering of galaxies. *Mon. Not. R. Astron. Soc.* **2013**, *429*, 1514–1528.
70. Ma, C.P.; Berschinger, E. Cosmological perturbation theory in the synchronous and conformal Newtonian gauges. *Astrophys. J.* **1955**, *455*, 7–25.
71. Kodama H.; Sasaki M. Cosmological Perturbation Theory. *Prog. Theor. Phys.* **1984**, *78*, 1–166.
72. Hu, W. Structure Formation with Generalized Dark Matter. *Astrophys. J.* **1998**, *506*, 485–494.
73. Luongo, O.; Quevedo, H. A unified dark energy model from a vanishing speed of sound with emergent cosmological constant. *Int. J. Mod. Phys. D* **2014**, *23*, 1450012.
74. Lewis, A.; Challinor, A.; Lasenby, A. Efficient computation of CMB anisotropies in closed FRW models. *Astrophys. J.* **2000**, *538*, 473–476.
75. Lewis, A.; Bridle, S. Cosmological parameters from CMB and other data: A Monte-Carlo approach. *Phys. Rev. D* **2002**, *66*, 103511.
76. Moresco, M.; Pozzetti, L.; Cimatti, A.; Jimenez, R.; Maraston, C.; Verde, L.; Thomas, D.; Citro, A.; Tojeiro, R.; Wilkinson, D. A 6% measurement of the Hubble parameter at $z \sim 0.45$: Direct evidence of the epoch of cosmic re-acceleration. *arXiv* **2016**, arXiv:1601.01701.
77. Aviles, A.; Gruber, C.; Luongo, O.; Quevedo, H. Cosmography and constraints on the equation of state of the Universe in various parametrizations. *Phys. Rev. D* **2012**, *86*, 123516.
78. Xu, L.; Wang, Y. Cosmography: Supernovae Union2, Baryon Acoustic Oscillation, Observational Hubble Data and Gamma Ray Bursts. *Phys. Lett. B* **2011**, *702*, 114–120.



© 2017 by the authors. Licensee MDPI, Basel, Switzerland. This article is an open access article distributed under the terms and conditions of the Creative Commons Attribution (CC BY) license (<http://creativecommons.org/licenses/by/4.0/>).